Impact of nanometer-thin stiff layer on adhesion to rough surfaces

Shubhendu Kumar,[1] Babu Gaire,[1] B. N. J. Persson,[2,3] and Ali Dhinojwala[1,*]
[1]*School of Polymer Science and Polymer Engineering, The University of Akron, Akron, Ohio 44325, USA*
[2]*Peter Grünberg Institute (PGI-1), Forschungszentrum Jülich, 52425 Jülich, Germany*
[3]*Multiscale Consulting, Wolfshovener Str. 2, 52428 Jülich, Germany*

(Received 26 February 2024; accepted 5 June 2024; published 2 July 2024)

Adhesives require molecular contact, which is governed by roughness, modulus, and load. Here, we measured adhesion for stiff glassy polymer layers of varying thickness on top of a soft elastomer with rough substrates. We found that a 90-nm-thick PMMA layer on a softer elastic block was sufficient to drop macroscopic adhesion to almost zero during the loading cycle. This drop in adhesion for bilayers follows the modified Persson-Tosatti model, where the elastic energy for conformal contact depends on the thickness and modulus of the bilayer. In contrast, we observed no dependence on thickness of the PMMA layer on the work of adhesion calculated using the pull-off forces. Understanding how mechanical gradients (like bilayers) affect adhesion is critical for areas such as adhesion, friction, and colloidal and granular physics.

DOI: 10.1103/PhysRevResearch.6.033015

I. INTRODUCTION

Adhesion between two surfaces requires molecular contact, and even a small roughness disrupts this molecular contact; this phenomenon is commonly known as the *adhesion paradox* [1–3]. Surfaces with low modulus can deform under pressure to create molecular contact [4,5]. However, achieving conformability requires additional energy for elastic deformation, which reduces the work of adhesion during approach [6]. When this additional elastic energy exceeds the intermolecular work of adhesion, a complete loss of macroscopic adhesion is observed, and the actual (or nominal) contact area is then dominated by Hertzian mechanics [7]. The mathematical formulation for calculating the effective work of adhesion was proposed by Persson and Tosatti in 2001 using height power spectral density (PSD), and this model has been validated for soft elastomeric siloxane polymers in contact with hard diamond surfaces by Dalvi *et al.* [8,9].

Many natural and manmade surfaces have gradient mechanical properties [10–12]. These mechanical gradients may result from differences in the composition or topological differences that result in an effective modulus that is a function of thickness [10–14]. For example, geckos have setae that branch into finer spatula and produce mechanical gradients controlled by both chemical composition and differences in physical parameters such as the diameter and length of the spatula as compared to setae [13,15]. These chemical or mechanical gradients can range from nanometer to micrometer scale and, in some cases, they help or deter mechanical contact. Such gradients offer an exquisite approach for controlling molecular contact and, thus, adhesion and friction [16].

Here we address the fundamental question of how a mechanical gradient can affect adhesion in contact with rough surfaces. To simplify the system, we considered a bilayer system with a high-modulus, glassy polymer poly (methyl methacrylate) (PMMA) on top of a soft elastomer poly dimethyl siloxane (PDMS), where the thickness of PMMA ranged between 10 and 90 nms. We measured the adhesion using the Johnson-Kendall-Roberts (JKR) technique by bringing the bilayer into contact with a sapphire hemispherical lens during approach and retraction. We compared the experimental results with predictions of the Persson-Tosatti model modified for bilayers [17]. An understanding of how adhesion is affected by mechanical gradients will shed light on the design principles of biological structures and inform the design of effective adhesives that can improve adhesion by controlling the effective modulus of the topmost layer in many applications including robotics and the biomedical sciences [12,16,18].

II. RESULTS AND DISCUSSION

Figure 1 summarizes the adhesion results for bilayers with PMMA thickness in the range of 10–84 nanometers. Fig. 1(a) illustrates the JKR geometry used to measure the bilayer adhesion. A sapphire lens with a radius of curvature of 1.25 mm is brought into contact with the bilayer at a speed of 60 nm/s and the contact area as a function of load is measured in a semi-static way; the results are shown in Fig. 1(b) for 10-, 40- and 84-nm-thick PMMA layers. The JKR theory, which was originally derived for two smooth homogenous surfaces, is also applicable for a bilayer geometry as shown by Johnson *et al.* [19] For this layered system in contact with rough surfaces, we have to consider the elastic deformation

*Contact author: ali4@uakron.edu

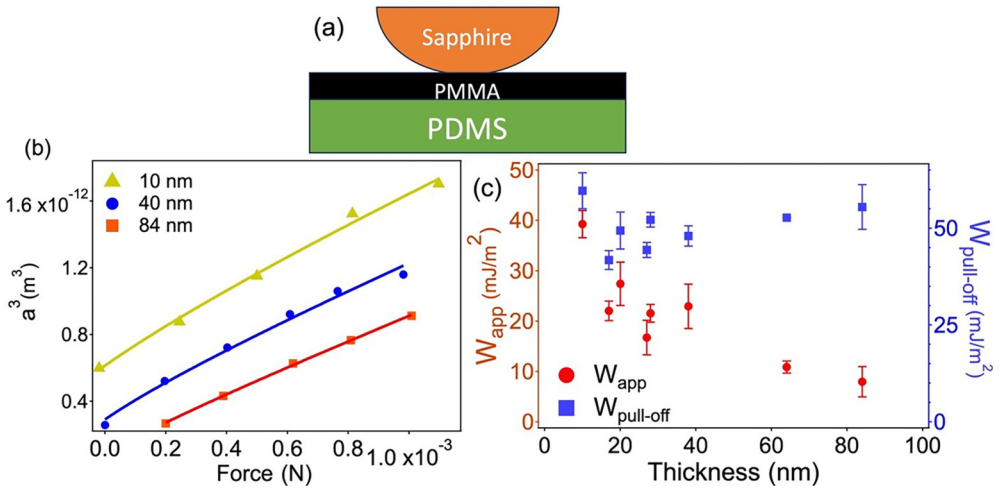

FIG. 1. (a) The geometry showing a sapphire lens brought in contact with a bilayer sample consisting of a top layer of rigid/glassy PMMA on a soft PDMS elastomer. The lens in contact with a flat sheet is used for JKR experiments in which the contact area is measured as a function of applied load. (b) Contact radius cubed vs applied force data for bilayer samples having PMMA layers with different thicknesses. The solid line is fit using the JKR contact mechanics model. (c) Plot of adhesion values obtained from JKR fits during approach (W_{app}; shown as red symbols). Pull-off ($W_{pull\text{-}off}$) values were determined by retracting the sapphire lens with a speed of 60 nm/s and using the JKR analysis (shown by blue symbols).

of the polymer sheet (U_{el}(polymer)) and the elastic energy to conform to the surface roughness of the lens (U_{el}(roughness)). This U_{el}(polymer) term has elastic contributions from both the top thin PMMA film and the thicker elastic PDMS sheet. The conservation of energy can be used to relate the total work (U_T) to form a contact as follows:

$$U_T = U_{el}(\text{polymer}) + U_{el}(\text{roughness}) - W_{true}A_{true}. \quad (1)$$

In Eq. (1), W_{true} is the true thermodynamic work of adhesion and A_{true} is the actual area of contact. In the JKR analysis, the U_{el}(roughness) term is not included, and we can combine the true work of adhesion and elastic energy to conform to the rough surface and refer to this as the apparent work of adhesion (W_{app}):

$$U_T = U_{el}(\text{polymer}) - W_{app}A_{app}. \quad (2)$$

This gives the relationship between the apparent and true work of adhesion:

$$W_{app}A_{app} = W_{true}A_{true} - U_{el}(\text{roughness}). \quad (3)$$

The U_{el}(roughness) can be calculated using the modified Persson-Tosatti equation (as discussed later). In Eqs. 2 and 3, A_{app} is the projected area. In the JKR equation, the effective modulus will include the contributions from elastic deformation of both the thin PMMA sheet and the much thicker, soft PDMS elastomer. Since PMMA films are much thinner than the PDMS elastomer sheets, the effective modulus will be closer to that of PDMS. In the Supplemental Material, we discuss the energy required to deform the PDMS sheet and the bending and stretching of the PMMA films (see Supplemental Material [20]). Thus, the current data can be modeled using the JKR model to determine the apparent work of adhesion [19,27].

The solid lines in Fig. 1(b) are the fit using the JKR equation to determine the apparent work of adhesion (W_{app}), and the effective moduli determined from the fits are summarized in Table S1 (See Supplemental Material [20]). During retraction, we measured the pull-off force and, using the JKR equation, we related the pull-off forces to the work of adhesion during pull-off ($W_{pull\text{-}off}$). Both of these values are plotted as a function of film thickness in Fig. 1(c). The values of W_{app} drop rapidly as we increase the thickness (Pearson correlation coefficient of −0.84). In comparison, the values of $W_{pull\text{-}off}$ are not affected by PMMA thickness (Pearson correlation coefficient of 0.27).

To determine W_{app} for the bilayers, the original Persson–Tosatti formalism was modified to account for changes in surface/interfacial energies of the PMMA (γ_1) and PMMA–PDMS (γ_{01}) interfaces. In addition, we needed to account for the effective elastic energy to conform to the roughness of the solid surface [8]. Figure 2 shows the steps involved in the development of the model to calculate W_{app}. Here, A_{app} is the projected area, γ_2 is the surface energy of the rough solid surface, and U_{el} is the elastic energy to deform the bilayer to conform to the rough solid surface [same as U_{el} (roughness) in Eqs. (1–3)]. Also, $W_{int} = \gamma_1 + \gamma_2 - \gamma_{12}$. W_{app} can be calculated based on the energy difference to separate the two surfaces:

$$W_{app} = W_{int}A_{true}/A_{app} - (\gamma_1 + \gamma_{01})\left(A_{true}/A_{app} - 1\right) - U_{el}/A_{app}. \quad (4)$$

To determine the change in surface energy in Eq. (4) due to the 0–1 interface, we have assumed that the 0–1 interface has the same PSD as the 1–2 interface after conformal contact, independent of film thickness. This is strictly true only for long wavelength roughness with the wavelength $\lambda \gg d$ (where d is the film thickness). For the bilayers studied here, γ_{01} is small and the accuracy of this assumption does not influence the adhesion values. The first two terms in Eq. (4)

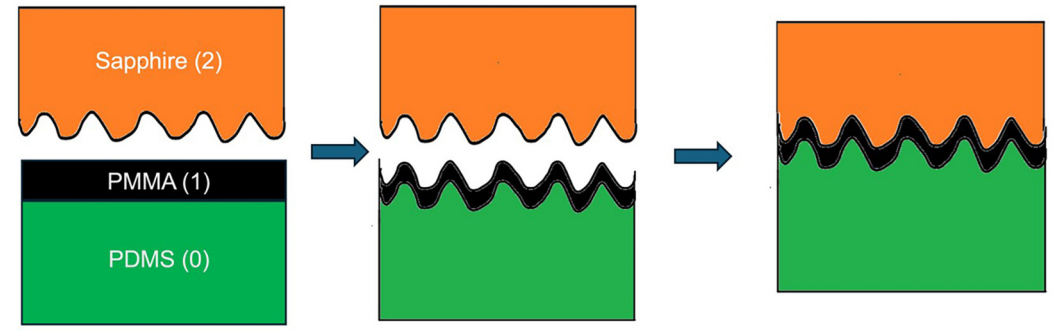

FIG. 2. Schematic showing different stages of a bilayer sample as it conforms to the roughness of the solid sapphire substrate. The center panel shows the intermediate stage to illustrate that the bilayer must deform to match the contours of the rough surface. The final panel shows a conformal contact with the rough surface. The equations provide the total energy of the system in each stage and the apparent work of adhesion is the difference between the final and the initial stage.

are also $W_{\text{true}}A_{\text{true}}/A_{\text{app}}$ in Eqs. (1) and (3). The elastic energy can be determined using the PSD of the rough surface, $C(q)$ (the definition of C is based on Ref. [28]):

$$\frac{U_{\text{el}}}{A_{\text{app}}} = E_1^* \frac{\pi}{2} \int_{q_0}^{q_1} dq q^2 \frac{C(q)}{S(q)}. \tag{5}$$

In Eq. (5), $E_1^* = E_1/(1-\nu_1^2)$ is the modulus of layer 1 (top layer) and $S(q)$ is the dimensionless surface responsive function, which depends on qd. The q in Eq. (5) is the wavevector (which is equal to $2\pi/\lambda$, where λ is the wavelength of roughness), and d is the thickness of the top layer. $S(q)$ also depends on the Poisson ratio of two layers (ν_o and ν_1) and the ratio of Young's moduli of the top and bottom layer (E_1/E_0) [17]

$$S(q) = \frac{1 + 4mqde^{-2qd} - mne^{-4qd}}{1 - (m + n + 4mq^2d^2)e^{-2qd} + mne^{-4qd}}. \tag{6}$$

The parameters m *and* n are expressed as follows:

$$m = \frac{\mu_1/\mu_0 - 1}{\mu_1/\mu_0 + 3 - 4\upsilon_1} \tag{7}$$

and

$$n = 1 - \frac{4(1-\upsilon_1)}{1 + (\mu_1/\mu_0)(3 - 4\upsilon_0)}, \tag{8}$$

where the shear moduli are related to Young's modulus: $\mu_0 = E_0/(2(1+\upsilon_0))$ and $\mu_1 = E_1/(2(1+\upsilon_1))$.

The value of $S(q)$ as a function of q for PMMA/PDMS in contact with the sapphire substrate is provided in Fig. S1 (See Supplemental Material [20]). As d tends to zero, Eq. (4) will converge to the value expected for a PDMS (layer 0) in contact with a rough substrate. As d tends to infinity, Eq. (4) will converge to the expected value for PMMA (layer 1).

To predict W_{app} for the system, we need to measure $C(q)$ for the sapphire lens and the PMMA–PDMS bilayer. Figure 3(a) shows the PSD for these two surfaces and the effective PSD depends mainly on the roughness of sapphire lens, since the bilayers are much smoother in comparison. The other parameters used to calculate W_{app} using Eqs. (4)–(8) are provided in Table S2 (See Supplemental Material [20]). The only unknown W_{int} is the intrinsic work of adhesion between the PMMA layer and the sapphire lens. The value for W_{int} of 49 mJ/m^2 was determined by minimizing the least squared error. Recent studies suggest that the modulus of PMMA could be a function of thickness [29,30] Accounting for this results in slightly higher values of adhesion for lower thickness and those results are summarized in Fig. S2 (See Supplemental Material [20]).

The theoretical predictions of W_{app} are shown in Fig. 3(b) as a function of film thickness (circles). The contribution of the surface area terms and the elastic energy in Eq. (4) are plotted in Fig. S3 (See Supplemental Material [20]). The second term is much smaller in magnitude because the area ratio term ($A_{\text{true}}/A_{\text{app}}$) is close to 1 for these almost smooth sapphire lenses. When the elastic contribution exceeds W_{int}, the adhesion drops to zero. The initial drop in W_{app} measured experimentally matches well with the theoretical predictions for smaller thicknesses. However, the W_{app} from the experiment dropped off more slowly than predicted by theory. One reason for these discrepancies may be due to the extreme sensitivity of W_{app} to roughness. For example, if we take the standard deviation based on different measurements of PSD of the sapphire lens and calculate W_{app}, we observe the predictions are spread out in the shaded region predicted by the bilayer model. This finding is intriguing because the results suggest that the sensitivity to roughness is a function of the thickness of the PMMA layer. Another reason for a slower drop in adhesion could be due to plastic deformation of PMMA film.

In Fig. 3(c) we plot the ratio of $U_{\text{el}}(q_{\text{cut}})/U_{\text{el (total)}}$ as a function of q_{cut}. For this calculation, we had to extrapolate the PSD to higher q values beyond the limit we measured experimentally. We found that for thinner film, this ratio converges to 1.0 at higher q values than that for a thicker film. Therefore, the variation in the roughness of the sapphire lens at lower q values (or larger wavelengths) affects the thicker film more than the thinner film, producing higher standard deviations. However, identifying specific reasons for deviation for thicker PMMA films will require a much more uniform rough surface with very little variation in roughness at lower q values.

The application of Eq. (4) to explain the adhesion results assumes that for all these samples, the contacts are conformal. The Persson-Tosatti model is only exact and applicable for conformal contact. We used surface-sensitive infrared-visible

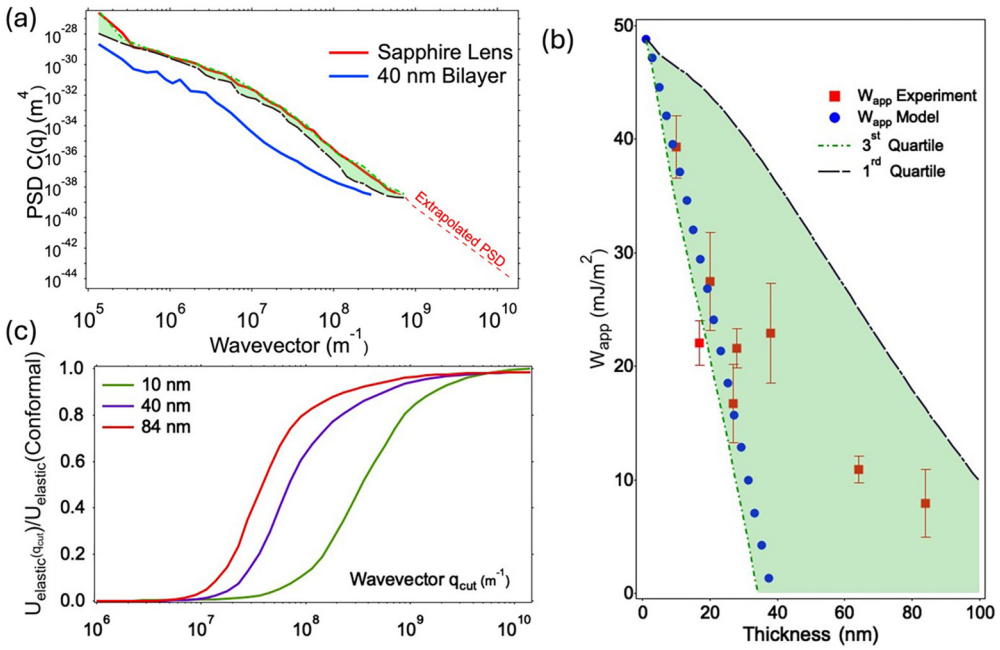

FIG. 3. Comparison of adhesion values measured experimentally and those predicted using the modified Persson-Tosatti [Eq. (4)]. (a) Results for the PSD (C) of the sapphire lens and a 40-nm-bilayer system. The shaded region represents variation in PSD of the sapphire lens within the interquartile range where the green dotted line represents the third quartile and the black dotted line represents the first quartile. The dotted red line represents the extrapolated average (C) of the sapphire lens. These profiles were measured using an atomic force microscope, and PSD was calculated using a previously published procedure [31,32]. (b) The experimental adhesion values for the bilayers in contact with sapphire are plotted as a function of thickness and are compared with the theoretical values predicted using Eqs. (1)–(5). The blue circles used the average values of C, and the shaded regions are calculated using the interquartile range of C (first and third quartile). (c) The ratio of elastic energy spent by several bilayer systems as a function of q_{cut}. These values are normalized by $U_{elastic}$ after integrating Eq. (5) with $q_l = 10^{10}$ (m^{-1}).

sum frequency generation (SFG) spectroscopy to address this question. Using SFG we measured the shift of the vibrational peak of the OH groups on the sapphire surface after contact with the PMMA surface using a bilayer geometry. This shift is due to hydrogen bonding between surface OH groups and carbonyl groups in PMMA, which is sensitive to variation in separation of less than 0.3–0.4 nm [33,34]. We observed no differences in the shift of the SFG peak for surface OH between the 10- or 200-nm-thick PMMA bilayers and no differences as a function of the applied load. The SFG results are summarized elsewhere [35]. This confirms that in these thickness ranges, the contact is conformal,and that Eq. (4) is applicable for modeling the adhesion data.

Finally, we explain the insensitivity of $W_{\text{pull-off}}$ to the thickness of the PMMA layer and why the trends are different from those observed for W_{app}. For smooth (ideal) surfaces, the JKR model should show similar values in approach and retraction (like Young's equation for contact angles). This has been observed for two bodies interacting with van der Waals interactions and smooth surfaces (mostly hydrophobic-hydrophobic contact interfaces). In most cases, one observes adhesion hysteresis, where the adhesion energy calculated during approach is lower than those obtained during retraction [36]. In these experiments, we have used a nonhysteretic PDMS sheet covered with a layer of glassy PMMA film in contact with a sapphire lens. The differences in adhesion values measured during approach and retraction are different, and we believe that viscoelasticity has a negligible impact on hysteresis. Also, previous studies have pointed out that high-molecular-weight PMMA (above the entanglement molecular weight) should resist damage and interdiffusion and, thus, should not contribute to adhesion hysteresis [37].

The other cause of hysteresis is roughness. We have previously reported deviation from the JKR model during the retraction cycle for homogeneous surfaces (not bilayers) in contact with rough diamond surfaces having low surface energy [9] We showed that the approach data matched with the Persson-Tosatti model, while the retraction data did not match this model. We observed contact pinning during retraction, and the energy dissipated during the adhesion cycle is instead proportional to the contact area. The slope of excess energy plotted as a function of the true contact area is similar to the thermodynamic work of adhesion. We referred to this process as a Griffith-like process for PDMS in contact with rough diamond surfaces.

Similarly, we can also explain the data here because of contact line pinning, where the adhesion energy is the product of the real contact area and the W_{int}. The W_{int} value for all of these thicknesses is dictated by PMMA–sapphire interaction, and they are similar for all measurements. The long-range van der Waals interaction is almost independent of the thickness of the PMMA layer. (Fig. S4, See Supplemental Material [20]) [38,39]. Based on our SFG results, we concluded that these samples are conformal and, since both W_{int} and the real contact area are not a function of the thickness of the PMMA layer,

we expect $W_{\text{pull-off}}$ to be a constant, in agreement with our experimental results.

A more extensive model was published recently to explain the contact of a soft homogeneous elastomer in contact with rough diamond surfaces and the impact of pinning of contact lines during retraction [40]. The pinning of the contact line leads to a higher adhesion when breaking a soft contact than was needed to form it, even in the absence of material-specific dissipation. Roughness peaks increase local adhesion, which pins the contact lines and increases the pull-off forces, and they may also explain why we observed $W_{\text{pull-off}}$ values that are independent of thickness and are higher than those measured during approach.

Lastly, we compare the experimental results with a semi-empirical model proposed by Ciavarella [41]. This model was developed based on Guduru's model for single wavelength asperities [42,43]. This model was adapted for multiple roughness described using a PSD to explain the adhesion data during approach and retraction for a single-layer PDMS substrate in contact with rough diamond surfaces [9,44]. In this model, a modified Johnson parameter [41,45] is used with U_{el} term based on Persson-Tosatti model for conformal contact. To compare the experimental results for bilayers with this model, we have used the U_{el} term shown in Eq. (5). The equations used to predict adhesion energy and the results comparing the adhesion during approach and retraction (Fig. S5) are provided in the Supplemental Material [20]. The approach data fits well with this model using $W_{\text{int}} = 62.5\,\text{mJ/m}^2$. However, it was not possible to obtain a good fit for retraction using the model proposed by Ciavarella by varying W_{int}.

In summary, we show that adhesion is extremely sensitive to the bilayer thickness in contact with solids of modestly low roughness. In the range in thickness between 10 and 90 nm, the adhesion during approach is lost due to roughness, as the elastic energy to conform to roughness is comparable to the intrinsic thermodynamic work of macroscopic adhesion. The predictions using a conformal bilayer contact model compare well with the experimental results and point towards extreme sensitivity of adhesion to small differences in roughness. These results provide insights on the control of adhesion by controlling the near-surface chemistry and modulus. For example, the model presented here can also predict how adhesion can be improved in contact with rough surfaces by layering a thin film of low-modulus polymers on a rigid polymer underlayer. This finding has a direct impact in many fields including soft robotics as well as adhesives for engineering and biomedical applications.

III. MATERIALS AND METHODS

Poly(methyl methacrylate) (PMMA) with a molecular weight of 100 000 g/mol and a polydispersity of 1.09 was purchased from Scientific Polymer Products. Different concentrations of PMMA samples were dissolved in toluene and spun coated to prepare PMMA films of thickness ranging from 10 to 84 nms. These films were dried at room temperature for 48 h before preparing the bilayer samples. Sheets of polydimethylsiloxane (PDMS) were prepared based on the procedure described by Dalvi *et al.* [9] PDMS sheets were Soxhlet-extracted using toluene at 124 °C for 72 h to remove any unreacted PDMS. After 24 h of drying in air, the PDMS sheets were dried under vacuum at 120 °C overnight to remove any remaining toluene. The PMMA films were transferred on top of the PDMS sheets using a previously reported film transfer procedure [33]. The PMMA films adhere to PDMS by van der Waals interactions. Hemispherical sapphire lenses (2.5 mm in diameter) were purchased from Edmund Optics. All chemicals were used as received.

IV. ADHESION MEASUREMENT

The adhesion experiment was done using the custom-built Johnson-Kendall-Roberts (JKR) test setup, in which a sapphire lens of diameter 2.5 mm was brought in contact with the bilayer system as shown in Fig. 1(a). The load and contact area were measured simultaneously until the maximum load of 1 mN. The apparent work of adhesion (W_{app}) was calculated by fitting contact area versus force data to the JKR equation [fitting results shown in Fig. 1(b)]. Once the maximum load was applied, the sapphire lens was retracted at the same speed, and the pull-off force was recorded. The pull-off force was then used to calculate the pull-off work of adhesion ($W_{\text{pull}-\text{off}}$) [21].

V. ROUGHNESS MEASUREMENT

Roughness for the spherical lens and the 40-nm bilayer film were measured by atomic force microscopy (AFM) using a Bruker Dimension Icon microscope. For the spherical lens, a total of 28 scans with scan sizes of 100 nm, 250 nm, 500 nm, 750 nm, 1 μm, 5 μm 10 μm, 25 μm and 50 μm were collected using Tap DLC 150 tips, which have a radius of less than 15 nm, a force constant of 5 N/m, and a resonance frequency of 150 kHz. A different tip, a RTESPA 300 tip with a nominal tip radius of 8 nm was used for measuring the roughness of the bilayer films. The AFM images were uploaded to a website known as Contact Engineering [46] to calculate the one-dimensional power spectra density (PSD), which was later converted to a two-dimensional PSD and then to a Persson's PSD (C) using the equations provided in Refs. [9,31,32]. The C data were used to calculate the elastic energy using Eq. (5).

ACKNOWLEDGMENTS

The authors thank P. Karanjkar, Dr. F. Cassin (University of Pittsburgh), and Prof. T. Jacobs (University of Pittsburgh) for their help with AFM measurements. In addition, we thank U. Patil, Dr. S. Merriman, and Dr. N. Kumar for their helpful comments and discussion. The authors acknowledge financial support for this work from the National Science Foundation (DMR-2208464). A.D. also acknowledges the financial support from the Knight Foundation (W. Gerald Austen Endowed Chair).

[1] K. L. Mittal, The role of the interface in adhesion phenomena, Polym. Eng. Sci. **17**, 467 (1977).

[2] G. Fourche, An overview of the basic aspects of polymer adhesion. Part I: Fundamentals, Polym. Eng. Sci. **35**, 957 (1995).

[3] A. Tiwari, J. Wang, and B. N. J. Persson, Adhesion paradox: Why adhesion is usually not observed for macroscopic solids, Phys. Rev. E **102**, 042803 (2020).

[4] B. N. J. Persson, Adhesion between elastic bodies with randomly rough surfaces, Phys. Rev. Lett. **89**, 245502 (2002).

[5] K. N. G. Fuller and David Tabor, The effect of surface roughness on the adhesion of elastic solids, Proc. R. Soc Ser. A **345**, 327 (1975).

[6] K. Kendall, Adhesion: Molecules and mechanics, Science **263**, 1720 (1994).

[7] H. Hertz, Ueber die berührung fester elastischer körper, Cell **1882**, 156 (1882).

[8] B. N. J. Persson and E. Tosatti, The effect of surface roughness on the adhesion of elastic solids, J. Chem. Phys. **115**, 5597 (2001).

[9] S. Dalvi, A. Gujrati, S. R. Khanal, L. Pastewka, A. Dhinojwala, and T. D. B. Jacobs, Linking energy loss in soft adhesion to surface roughness, Proc. Natl. Acad. Sci. USA **116**, 25484 (2019).

[10] H. Peisker, J. Michels, and S. N. Gorb, Evidence for a material gradient in the adhesive tarsal setae of the ladybird beetle *Coccinella septempunctata*, Nat. Commun. **4**, 1661 (2013).

[11] S. Flenner, C. F. Schaber, I. Krasnov, H. Stieglitz, M. Rosenthal, M. Burghammer, S. N. Gorb, and M. Müller, Multiple mechanical gradients are responsible for the strong adhesion of spider attachment hair, Adv. Mater. **32**, 2002758 (2020).

[12] J. L. Schäfer, T. Meckel, S. Poppinga, and M. Biesalski, Chemical gradients in polymer-modified paper sheets—towards single-layer biomimetic soft robots, Biomimetics **8**, 43 (2023).

[13] X. Dong, R. Zhang, Y. Tian, M. A. Ramos, T. S. Hu, Z. Wang, H. Zhao, L. Zhang, Y. Wan, Z. Xia *et al.*, Functionally graded gecko setae and the biomimics with robust adhesion and durability, ACS Appl. Polym. Mater. **2**, 2658 (2020).

[14] Y. Zhang, W. Zhao, S. Ma, H. Liu, X. Wang, X. Zhao, B. Yu, M. Cai, and F. Zhou, Modulus adaptive lubricating prototype inspired by instant muscle hardening mechanism of catfish skin, Nat. Commun. **13**, 377 (2022).

[15] H. Gao, X. Wang, H. Yao, S. Gorb, and E. Arzt, Mechanics of hierarchical adhesion structures of geckos, Mech. Mater. **37**, 275 (2005).

[16] E. Arzt, H. Quan, R. M. McMeeking, and R. Hensel, Functional surface microstructures inspired by nature–from adhesion and wetting principles to sustainable new devices, Prog. Mater Sci. **120**, 100823 (2021).

[17] B. N. J. Persson, Contact mechanics for layered materials with randomly rough surfaces, J. Phys.: Condens. Matter **24**, 095008 (2012).

[18] C. He, X. Xu, Y. Lin, Y. Cui, and Z. Peng, A bilayer skin-inspired hydrogel with strong bonding interface, Nanomaterials **12**, 1137 (2022).

[19] K. L. Johnson and I. Sridhar, Adhesion between a spherical indenter and an elastic solid with a compliant elastic coating, J Phys D **34**, 683 (2001).

[20] See Supplemental Material at http://link.aps.org/supplemental/10.1103/PhysRevResearch.6.033015 for details on JKR applicability, tabular experimental data, model parameters, comparison of model with effects of variation in modulus of PMMA with thickness, comparison of different component of Eq. (4), variation in the Lifshitz–van der Waals contributions to the adhesion energy as a function of the thickness of PMMA, Ciavarella model and its comparison with experimental adhesion values, which includes Refs. [21–26].

[21] K. L. Johnson, K. Kendall, and A. D. Roberts, Surface energy and the contact of elastic solids, Proc. R. Soc. London Ser. A **324**, 301 (1971).

[22] E. M. Lifshitz and L. D. Landau, *Theory of Elasticity*, 2nd ed. (Pergamon Press, Oxford, 1975).

[23] J. E. Mark, editor, *Physical Properties of Polymers Handbook*, 2nd ed. (Springer Science + Business Media, New York, 2007).

[24] V. S. Mangipudi, E. Huang, M. Tirrell, and A. V. Pocius, Measurement of interfacial adhesion between glassy polymers using the JKR method, Macromol. Symp. **102**, 131 (1996).

[25] J. Chang, K. B. Toga, J. D. Paulsen, N. Menon, and T. P. Russell, Thickness dependence of the Young's modulus of polymer thin films, Macromolecules **51**, 6764 (2018).

[26] P. H. Mott, J. R. Dorgan, and C. M. Roland, The bulk modulus and Poisson's ratio of "incompressible" materials, J. Sound Vib. **312**, 572 (2008).

[27] F. K. Yang, W. Zhang, Y. Han, S. Yoffe, Y. Cho, and B. Zhao, Contact" of nanoscale stiff films, Langmuir **28**, 9562 (2012).

[28] B. N. J. Persson, O. Albohr, U. Tartaglino, A. I. Volokitin, and E. Tosatti, On the nature of surface roughness with application to contact mechanics, sealing, rubber friction and adhesion, J. Phys. Condens. Matter **17**, R1 (2005).

[29] C. M. Stafford, B. D. Vogt, C. Harrison, D. Julthongpiput, and R. Huang, Elastic moduli of ultrathin amorphous polymer films, Macromolecules **39**, 5095 (2006).

[30] J. M. Torres, C. M. Stafford, and B. D. Vogt, Elastic modulus of amorphous polymer thin films: Relationship to the glass transition temperature, ACS Nano **3**, 2677 (2009).

[31] T. D. B. Jacobs, T. Junge, and L. Pastewka, Quantitative characterization of surface topography using spectral analysis, STMP **5**, 013001 (2017).

[32] M. C. Röttger, A. Sanner, L. A. Thimons, T. Junge, A. Gujrati, J. M. Monti, W. G. Nöhring, T. D. B. Jacobs, and L. Pastewka, Contact.engineering—create, analyze and publish digital surface twins from topography measurements across many scales, Surf. Topogr. **10**, 035032 (2022).

[33] B. Gaire, M. C. Wilson, S. Singla, and A. Dhinojwala, Connection between molecular interactions and mechanical work of adhesion, ACS Macro Lett **11**, 1285 (2022).

[34] N. Kumar, S. Kaur, R. Kumar, M. C. Wilson, S. Bekele, M. Tsige, and A. Dhinojwala, Interaction geometry causes spectral line-shape broadening at the solid/liquid interface, J. Phys. Chem. C **123**, 30447 (2019).

[35] U. Patil, S. Merriman, S. Kumar, and A. Dhinojwala, Measurement of nanoscale interfacial contact area using vibrational spectroscopy, arXiv:2402.12697.

[36] A. Tiwari, L. Dorogin, A. I. Bennett, K. D. Schulze, W. G. Sawyer, M. Tahir, G. Heinrich, and B. N. J. Persson, The effect of surface roughness and viscoelasticity on rubber adhesion, Soft Matter **13**, 3602 (2017).

[37] G. D. Degen, T. R. Cristiani, N. Cadirov, R. C. Andresen Eguiluz, K. Kristiansen, A. A. Pitenis, and J. N. Israelachvili, Surface damage influences the JKR contact mechanics of glassy

low-molecular-weight polystyrene films, Langmuir **35**, 15674 (2019).

[38] J. N. Israelachvili, *Intermolecular and Surface Forces*, 3rd ed. (Academic Press, London, 2003).

[39] J. N. Israelachvili, The calculation of van der Waals dispersion forces between macroscopic bodies, Proc. R. Soc. London Ser. A **331**, 39 (1972).

[40] A. Sanner, N. Kumar, A. Dhinojwala, T. D. B. Jacobs, and L. Pastewka, Why soft contacts are stickier when breaking than when making them, Sci. Adv. **10**, eadl1277 (2024).

[41] M. Ciavarella, On roughness-induced adhesion enhancement, J. Strain Anal. Eng. Des. **51**, 473 (2016).

[42] P. R. Guduru, Detachment of a rigid solid from an elastic wavy surface: Theory, J. Mech. Phys. Solids **55**, 445 (2007).

[43] P. R. Guduru and C. Bull, Detachment of a rigid solid from an elastic wavy surface: Experiments, J. Mech. Phys. Solids **55**, 473 (2007).

[44] A. Papangelo and M. Ciavarella, A criterion for the effective work of adhesion in loading and unloading of adhesive soft solids from rough surfaces, Tribol. Lett. **69**, 9 (2021).

[45] K. L. Johnson, The adhesion of two elastic bodies with slightly wavy surfaces, Int. J. Solids Struct. **32**, 423 (1995).

[46] https://contact.engineering.